

The C star population of DDO 190^{★,★★}

P. Battinelli¹ and S. Demers²

¹ INAF, Osservatorio Astronomico di Roma, Viale del Parco Mellini 84, 00136 Roma, Italia
e-mail: battinel@oarhp1.rm.astro.it

² Département de Physique, Université de Montréal, CP 6128, Succursale Centre-Ville, Montréal, Québec H3C 3J7, Canada
e-mail: demers@astro.umontreal.ca

Received 7 February 2005 / Accepted 6 October 2005

ABSTRACT

We have carried out deep *R*, *I*, CN, TiO observations of the dwarf irregular galaxy DDO 190. We confirm the existence of an intermediate-age population around this galaxy. The identification of 47 carbon stars seen up to 5 arcmin from the centre of the galaxy implies that the population distribution of DDO 190 is similar to those found in some other Local Group dIrr galaxies. An estimate of the metallicity, $[Fe/H] = -1.55 \pm 0.12$, is obtained based on the observed C/M ratio. From the analysis of star counts, corrected for the radial variation of the incompleteness level, we determine a scale-length $\alpha = 40 \pm 5''$, in agreement with the recent literature.

Key words. galaxies: individual: DDO 190 – galaxies: dwarf – stars: carbon – stars: AGB and post-AGB – galaxies: fundamental parameters

1. Introduction

Dwarf galaxies play a crucial role in the CDM scenario for galaxy formation, having been suggested to be the natural building blocks from which larger structures are built up by merging processes. In this scenario dwarf galaxies are formed from small-scale density fluctuations in the primeval universe. In the present universe we observe at least two well defined topologies – dwarf Irregulars (dIrrs) and dwarf spheroidal/elliptical galaxies (dSph/dEs). These classes differ by their stellar content (essentially no young stars for dSph/dEs with the exception of a few well known cases such as NGC 205; presence of a conspicuous young component for the dIrrs), their gas content (no gas for dSph/dEs; conspicuous gas content often with the presence of surrounding huge HI clouds for dIrrs), their location in the universe (dSph/dEs concentrated in the high density regions of galaxy clusters; a fraction of the order of 50% of dIrrs are isolated galaxies). On the basis of such observational evidence, it has been suggested that these two classes have a common origin, dSph/dEs being the result of intensive gas stripping by massive neighbours that removed the gaseous component and thus halted the star formation long ago. On the other hand dIrrs, which avoid dense regions, exclusively followed their intrinsic evolution with no significant external influence. It is therefore reasonable to

expect signs of the gravitational collapse of the initial small amplitude perturbation still visible today around isolated dIrrs.

DDO 190 (also known as UGC 9240) is a Magellanic dwarf, of morphological type Im. It is well outside of the Local Group. Its distance has been determined, from the apparent magnitude of the Tip of the Red Giant Branch (TRGB), to be 2.9 ± 0.2 Mpc by Aparicio & Tikhonov (2000) and 2.79 ± 0.26 Mpc by Karachentsev et al. (2002). We adopt a distance to DDO 190 of 2.85 Mpc, that is the average of the above estimates. The total *V*-magnitude of DDO190 was determined by Prugniel & Héraudeau (1998) to be $V = 12.7$ corresponding to $M_V = -14.5$. The HI mass of DDO 190, estimated at $5 \times 10^7 M_\odot$ by Stil & Israel (2002a) is normal for a galaxy of its luminosity. For instance, WLM, a galaxy with the same total luminosity, hosts a total HI mass of $6.1 \times 10^7 M_\odot$ (Mateo 1998). The HI density map shows a maximum on the west side of the optical centre, its velocity field is somewhat irregular but rotation is clearly visible (Stil & Israel 2002b). The major axis of the HI has a PA = 150° and the HI disk is seen to a diameter of 200 arcsec.

Dwarf irregular galaxies are surrounded by old stellar halos (Vancevičius et al. 2004; Minniti et al. 2003). The existence of such *pure* old halos (i.e. made exclusively by 10+ Gyr old stars) represents therefore a crucial piece of evidence in favour of the bottom-up scenario of galaxy formation.

We find in the literature statements such as: “*extended structures lacking of young stars are being routinely discovered in dwarf irregulars*” (Hidalgo et al. 2003). However these assertions are still based on few galaxies and need to be confirmed.

* Based on observations obtained at the Italian Telescopio Nazionale Galileo.

** Table 2 is also available in electronic form at the CDS via anonymous ftp to [cdsarc.u-strasbg.fr](ftp://cdsarc.u-strasbg.fr) (130.79.128.5) or via <http://cdsweb.u-strasbg.fr/cgi-bin/qcat?J/A+A/447/473>

Edge-on spirals also show stellar density gradients along the z -axis, interpreted by Mould (2005) as being the signature of old and relatively metal-poor thick disks. For instance, our ongoing carbon star survey of Local Group dwarfs, based on the large format mosaic CFH12K ($42' \times 28'$), has revealed that three out of five dIrrs studied have stellar halos made of old *and* intermediate-age stars while the two others do not seem to possess any significant stellar halo. Surprisingly, these two galaxies, NGC 3109 and WLM, are among those claimed to retain a genuine halo-disk structure (Minniti et al. 1999; Minniti & Zijlstra 1996, 1997). Minniti et al. (1999) surveyed NGC 3109 only up to $4.5'$ from its major axis, thus interpreting the inclined thick disk as a halo. Likewise, our observations show clearly that the minor axis profile of WLM ends abruptly $5'$ from its centre. Furthermore, the discovery of intermediate-age stars in the halo of some dIrrs (IC 1613, Albert et al. 2000; NGC 6822, Letarte et al. 2002; IC 10, Demers et al. 2004) is strong evidence that the halos of dIrrs require more than a simple halo/disk scenario. At present, the existence of *pure* old halo needs to be confirmed. The reason why a tenuous intermediate-age halo component may have been missed by several authors is because they select stars in an inappropriate region on the CMD. Indeed, one is forced to select stars in a box *well above* the TRGB because the region just above the tip, where most of the AGB stars are located, is polluted by numerous blended giants (see e.g. Aparicio & Gallart 1995). An alternative approach that uses carbon stars as probes to trace the galactic halos has been proposed. For example, Letarte et al. (2002) have demonstrated that cool carbon stars (CN-type) can trace low density intermediate-age halos because they are seen against a zero foreground. It is thus necessary to observe a larger number of isolated dIrrs and investigate their structure.

Aparicio & Tikhonov (2000) report the existence of an old stellar halo in DDO 190. However, the integrated B and R luminosity profiles of DDO 190, observed by Bremnes et al. (1999), show a luminosity excess above a pure exponential in its surface brightness profile at large radii. This suggests the presence of two distinct galactic components which would imply that DDO 190 is similar to NGC 6822 or IC 10, thus making DDO 190 an interesting dwarf to revisit.

2. Observations and data reduction

The observations carried out at the Telescopio Nazionale Galileo were acquired during four consecutive nights in June 2004. They consist of images obtained through R , I , CN and TiO filters. The narrow-band ($FWHM = 30$ nm) CN and TiO filters are centred on 808.6 nm and 768.9 nm. The camera DOLORES is equipped with a Loral thinned and back-illuminated 2048×2048 CCD with a scale of 0.275 arcsec/px corresponding to a field of view of about 9.4×9.4 .

We observed one field centred at $\alpha = 14^{\text{h}}25^{\text{m}}01^{\text{s}}$, $\delta = +44^{\circ}28'33''$ (J2000.0) which is $3'$ south and $3'$ east of DDO 190. The galaxy is thus located in a corner of the field so to have, on the opposite corner, a good representation of the foreground and background field (see Fig. 1). The observing log is presented in Table 1; we have exposed for more than 6000 s in I and R . This represents, in terms of photons,

Table 1. Summary of the observations.

Filter	Exposure	\langle Airmass \rangle	\langle FWHM \rangle
I	11×600 s	1.15	0.81''
R	11×600 s	1.15	1.08''
CN	9×1200 s	1.08	0.90''
TiO	9×1200 s	1.10	0.98''

an improvement by a factor of four when compared to the Aparicio & Tikhonov (2000) observations. The galaxy has been observed nearly at the zenith and the seeing ranged from 0.8 to 1.1 arcsec.

After bias and flat-field corrections, instrumental magnitudes were obtained following the DAOPHOT-II, ALLSTAR and ALLFRAME pipeline (Stetson 1994). Calibration equations were provided by the TNG staff in the following form:

$$(R - I) = 0.9089(r - i) + 0.534 - k_{RI}X,$$

$$I = 0.899 + i + 0.1858(R - I) - k_I X.$$

We assume standard La Palma extinction coefficients and did not determine them for each night. The zero-point of the narrow band observations was obtained setting the average (CN–TiO) of *blue stars* equal to zero following a procedure similar to that adopted by Brewer et al. (1995). This procedure is explained in Letarte et al. (2002) and in the present paper we follow their definition of *blue stars* as stars in the colour range $0.0 < (R - I)_0 < 0.45$. To convert observed $(R - I)$ colours into intrinsic colours we adopt $A_I = 0.023$ and $A_R = 0.032$ (Schlegel et al. 1998) which give $E(R - I) = 0.009$.

3. Results

3.1. The colour–magnitude diagrams

Since DDO 190 is located at high galactic latitude ($b = 64.5^\circ$), the contamination by foreground stellar objects in the observed field is expected to be marginal while, as a consequence of the long integration time, background non-stellar objects induce a significant contamination. Most of the non-stellar objects present in the field have been removed setting a threshold for the DAOPHOT psf-fitting parameter SHARP. We limit our RI photometric catalogue to stars with errors smaller than $\sigma_{(R-I)} = 0.10$. A further effect influencing our catalogues is the severe crowding in the central region of the galaxy. Even though this study is focused on the nature of the stellar halo around DDO 190, it is important to determine the region where we have reliable colour–magnitude and colour–colour diagrams representing the galaxy. We therefore assume a centre and circular symmetry for DDO 190 (as justified in Sect. 3.6) and inspect the CMDs at various distances from the galaxy centre. Four concentric regions are defined (see Fig. 1).

The CMDs of these four annular regions are displayed in Fig. 2. The centre (panel a) is clearly affected by severe crowding: faint stars are missing and there is an excess of bright stars. In the annulus $150 < r(\text{px}) < 500$ the RGB of DDO 190 is evident and we consider this region to be representative of the galaxy. We denote this region as the “DDO 190 annulus”.

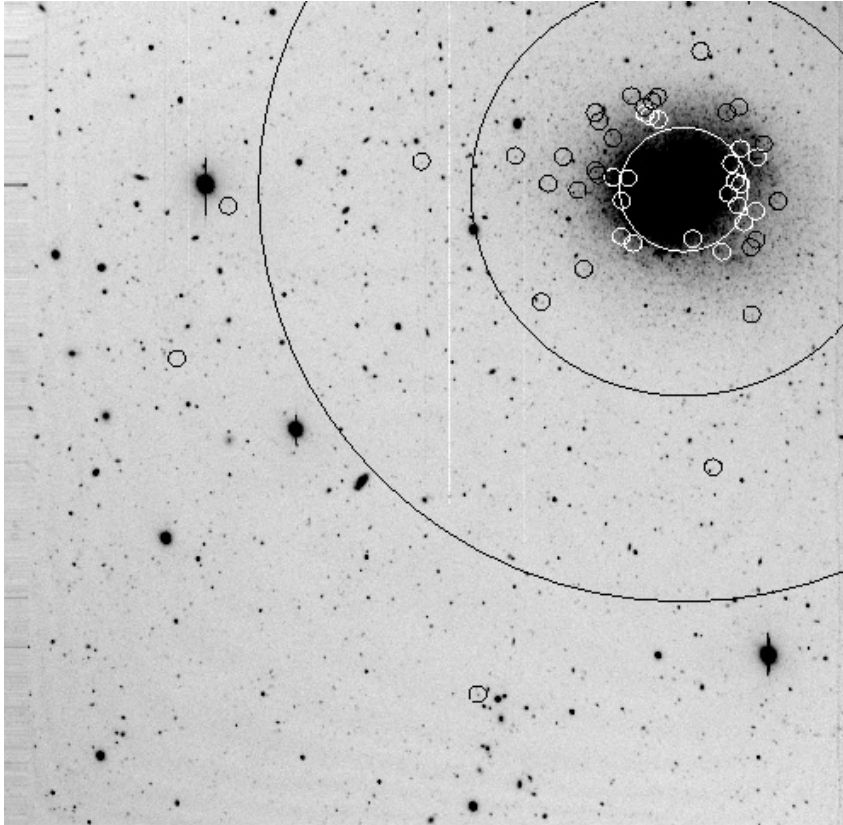


Fig. 1. Image of DDO 190 obtained by combining the 11 R exposures. Black/white circles surround the 47 C stars identified (in Sect. 4.1). Large circles limit the four regions defined in Sect. 3.1. The “DDO 190 annulus” is the region between the white circle and the first black circle. North is up and East to the left. The field of view is $9.4' \times 9.4'$.

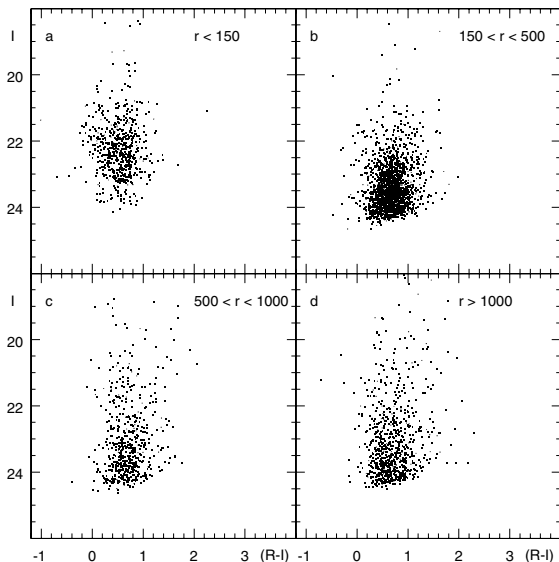


Fig. 2. Colour magnitude diagrams for four annular regions defined by the limits of the galactocentric distance r (in pixel units) given on the upper-right of each panel. For an easy comparison we used colour and magnitude limits as in Aparicio & Tikhonov (2000) Fig. 2.

Beyond the “annulus” we have, for $r(\text{px}) > 1000$, no evident feature and this is a field containing foreground Galactic stars

as well as background non-stellar objects not rejected by the SHARP condition. We will call this sample the “control area”. The region between the annulus and the control area is also featureless even though we cannot exclude the presence of a tenuous contribution by DDO 190 stars. The annulus, particularly in its inner part, is not free of blending. To evaluate the importance of such blending we divided the annulus into several subsamples (sub-annuli) and we determine the luminosity of the TRGB using a Sobel filter (weights: $-2, -1, 0, 1, 2$) applied to the I -luminosity function. For all the subsamples we obtain (within the errors) the same luminosity of $I_{\text{TRGB}} = 23.3$, in fair agreement with the value found by Aparicio & Tikhonov (2000). In Fig. 3 (top and central panels) the normalised luminosity functions and their Sobel convolutions for two subsamples of the annulus regions are shown. In the lower panel the same functions are plotted for the control area. We note that in the first two panels the position of the TRGB is the same and that some blending, seen as an excess of counts at magnitudes brighter than the tip, is evident in the inner region. In the control area the Sobel algorithm fails to detect any significant jump in the LF, as expected for an outer field.

3.2. The colour–colour diagrams

In Fig. 4 the colour–colour plots for the four samples defined in the previous section are presented. To minimize the

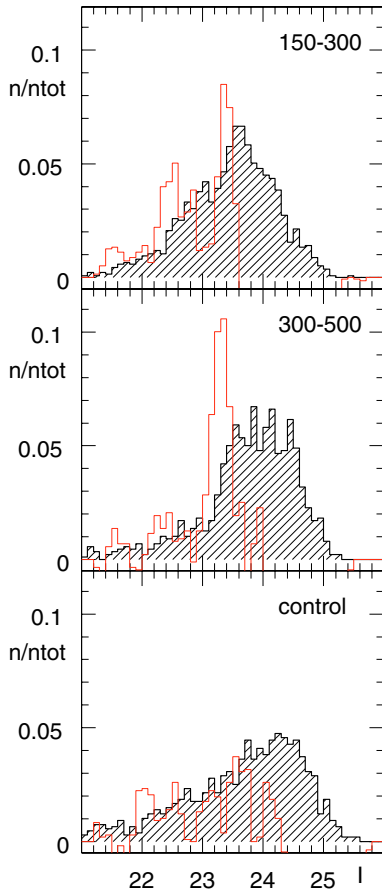


Fig. 3. Normalised luminosity functions (shaded histograms) and their Sobel convolutions for three different area (see text).

scatter we limit our R , I , CN, TiO catalogue to those stars for which $(\sigma_{(R-I)}^2 + \sigma_{(CN-TiO)}^2)^{1/2} < 0.10$. We have 1324 stars that satisfy this condition along with the sharpness condition introduced in the previous section. As explained in Albert et al. (2000), C stars and M stars can be separated in the $(CN - TiO) - (R - I)$ plane since they define two distinct sequences departing from the bulk of stars towards red colours with $(CN - TiO)$ colour indices of opposite sign: positive for C stars and negative for M stars. Therefore, the adoption of two boxes in the colour–colour plane (see Fig. 4) allows a straightforward identification of C and M stars. An inspection of the diagrams in Fig. 4 reveals that: *i*) C stars are seen in all four samples, even at large distances from the galaxy centre where few, if any, stars of DDO 190 are expected; *ii*) the sequence of M stars is visible only in the two outer fields (panel c and d) showing that DDO 190 is lacking very red giants. This point indicates that the metallicity of DDO 190 is quite low, as we will see in Sect. 4.3.

4. Discussion

At a distance of ~ 3 Mpc, DDO 190 is close to the limit of AGB surveys. Davidge (2003), using the Gemini Telescope, has shown that NGC 2403 (3.6 Mpc) has an intermediate-age population at large radii. An earlier attempt to survey this galaxy by Hudon et al. (1989) has revealed the existence of

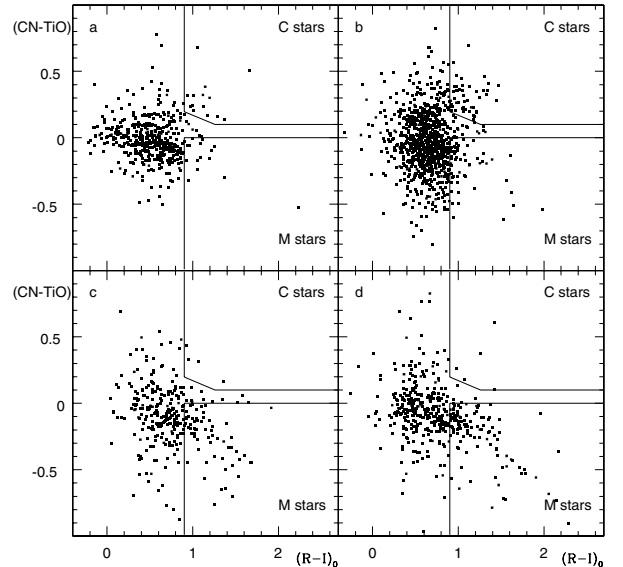


Fig. 4. Colour colour diagrams for the annular regions (same as Fig. 1) defined in Sect. 3.1.

some C stars while stressing the difficulties of investigating galaxies at such distances.

4.1. C stars

On the basis of the colour–colour plot we identify 47 C stars; their photometric properties along with J2000 equatorial coordinates and CCD coordinates are listed in Table 2. From the spatial distribution of these stars, shown in Fig. 1, we see that three C stars fall in the outermost region (#44, 46, 47) that we have previously considered as representative of the foreground/background contamination. We inspected carefully, on the combined images in all the four filters, the stellar images of these outer candidate C stars and found no evidence of bright neighbours or CCD defects, thus there is no reason to reject them.

Two of them (#46, 47) have colours that put them very close to the limits of the box defining the C star region (see Fig. 4d) and in principle might be “migratory” cases caused by the photometric errors (which however are quite small). The third object, which is also the outermost C star, has very a positive $(CN - TiO)$ colour and is located in the CMD well above the tip of the red giant branch. An opportunity to check the photometry and evaluate the relevance of the blurring in our DOLORES images is offered by a WFPC2 field centred on DDO 190 available from the HST archive. The data consist of two exposures of 600 s each in $F814W$ and $F606W$. Results from these observations are given by Karachentsev et al. (2002). We downloaded the two images and processed them with HSTphot (Dolphin 2000), kindly provided to us by the author. Pixel coordinates were translated into RA and Dec using the *metric* task in IRAF/STSDAS which also corrects the geometric distortions of each chip. In the HST field there are 21 of the 47 C stars we identified. These stars are all recovered when a cross identification between them and stars (brighter than $I = 23$ mag) found by HSTphot is performed.

Table 2. C stars of DDO 190.

id	RA	Dec	X	Y	I	σ_I	$R - I$	σ_{R-I}	CN-TiO	$\sigma_{\text{CN-TiO}}$
1	14 24 37.79	44 31 31.10	171.8	1467.9	22.720	0.020	1.297	0.036	0.356	0.042
2	14 24 38.68	44 32 07.70	205.9	1602.3	22.628	0.019	1.187	0.037	0.166	0.035
3	14 24 39.05	44 31 59.00	220.9	1570.9	21.858	0.012	1.139	0.019	0.388	0.020
4	14 24 39.07	44 31 05.60	223.4	1377.2	22.532	0.016	1.222	0.027	0.194	0.031
5	14 24 39.13	44 31 24.10	225.1	1444.2	22.515	0.017	1.062	0.027	0.217	0.033
6	14 24 39.31	44 30 16.90	234.3	1200.8	22.643	0.017	1.334	0.029	0.323	0.034
7	14 24 39.37	44 31 00.50	235.6	1359.1	22.543	0.017	1.224	0.026	0.190	0.032
8	14 24 39.82	44 31 16.50	252.7	1417.4	21.851	0.010	1.252	0.017	0.300	0.017
9	14 24 40.01	44 31 41.40	259.4	1508.1	22.671	0.021	1.178	0.037	0.167	0.039
10	14 24 40.07	44 32 04.10	260.8	1590.9	22.184	0.016	0.922	0.021	0.277	0.027
11	14 24 40.18	44 32 31.30	263.9	1690.0	22.571	0.017	1.186	0.027	0.134	0.034
12	14 24 40.20	44 31 27.50	267.4	1457.9	22.208	0.016	0.980	0.027	0.234	0.028
13	14 24 40.35	44 31 43.00	272.9	1514.5	21.950	0.018	0.942	0.025	0.318	0.026
14	14 24 40.62	44 31 54.40	282.8	1556.3	22.394	0.020	1.154	0.031	0.384	0.033
15	14 24 40.75	44 31 34.70	288.8	1484.9	22.605	0.024	1.140	0.044	0.235	0.050
16	14 24 40.91	44 32 27.50	293.2	1677.2	22.187	0.013	0.937	0.018	0.238	0.024
17	14 24 41.10	44 30 57.30	304.0	1349.2	22.432	0.016	1.088	0.026	0.215	0.030
18	14 24 41.56	44 28 36.80	325.3	840.7	23.493	0.038	0.959	0.052	0.325	0.084
19	14 24 42.52	44 33 06.30	354.8	1820.7	22.933	0.021	1.316	0.035	0.459	0.042
20	14 24 42.86	44 31 05.20	373.2	1379.5	23.188	0.036	1.127	0.058	0.321	0.070
21	14 24 44.99	44 32 21.80	454.3	1660.1	22.811	0.022	1.055	0.034	0.393	0.043
22	14 24 45.03	44 32 36.40	455.4	1713.5	22.099	0.012	0.927	0.017	0.201	0.025
23	14 24 45.34	44 32 33.70	467.8	1703.8	22.953	0.022	1.066	0.034	0.199	0.044
24	14 24 45.49	44 32 23.80	474.0	1667.7	22.712	0.018	1.061	0.029	0.394	0.038
25	14 24 45.77	44 32 25.40	485.0	1674.0	22.066	0.011	1.047	0.019	0.448	0.024
26	14 24 45.83	44 32 29.50	487.1	1688.9	23.488	0.039	1.198	0.063	0.161	0.077
27	14 24 46.41	44 31 01.50	513.3	1368.7	22.562	0.022	0.970	0.035	0.386	0.035
28	14 24 46.62	44 32 36.60	517.8	1715.3	22.506	0.017	1.073	0.025	0.225	0.035
29	14 24 46.77	44 31 43.70	526.0	1522.2	22.604	0.019	1.300	0.038	0.160	0.038
30	14 24 47.11	44 31 28.90	539.9	1468.8	22.018	0.016	1.013	0.025	0.205	0.030
31	14 24 47.13	44 31 06.00	541.3	1385.2	22.472	0.017	1.185	0.029	0.224	0.034
32	14 24 47.65	44 31 44.00	560.8	1523.8	21.533	0.009	0.949	0.017	0.567	0.019
33	14 24 47.66	44 32 09.40	560.2	1616.4	22.566	0.022	1.079	0.032	0.214	0.035
34	14 24 48.50	44 32 20.00	592.7	1655.5	22.623	0.019	0.982	0.026	0.382	0.037
35	14 24 48.54	44 31 45.40	595.8	1529.3	22.683	0.020	1.217	0.041	0.348	0.043
36	14 24 48.72	44 31 48.40	602.4	1540.3	21.765	0.010	1.072	0.015	0.320	0.018
37	14 24 48.78	44 32 25.70	603.5	1676.4	22.461	0.016	0.969	0.022	0.296	0.031
38	14 24 49.37	44 30 44.60	630.1	1308.3	22.372	0.013	1.363	0.022	0.410	0.032
39	14 24 49.77	44 31 35.70	644.3	1494.4	22.312	0.014	1.160	0.022	0.228	0.025
40	14 24 50.65	44 31 57.00	678.4	1572.4	22.665	0.019	0.990	0.025	0.354	0.035
41	14 24 51.53	44 31 39.70	713.3	1509.6	22.926	0.023	0.952	0.035	0.348	0.044
42	14 24 51.89	44 30 23.10	729.7	1230.6	22.710	0.019	1.079	0.027	0.271	0.039
43	14 24 53.53	44 31 57.50	791.3	1574.7	22.382	0.016	1.002	0.022	0.357	0.029
44	14 24 55.65	44 26 08.60	879.3	307.0	22.383	0.017	1.431	0.027	0.607	0.035
45	14 24 59.15	44 31 53.90	1012.3	1561.1	22.822	0.020	1.080	0.030	0.312	0.040
46	14 25 10.72	44 31 26.10	1466.9	1456.7	23.406	0.037	1.078	0.053	0.175	0.060
47	14 25 13.79	44 29 47.30	1587.6	1097.2	23.608	0.040	1.437	0.068	0.101	0.064

The magnitude comparison yields an average $\Delta I = 0.05$ mag, confirming the zero point of our photometry, and a dispersion of 0.3 mag, quite reasonable for C stars expected to be variable. We therefore conclude that even the photometry of the C stars identified in the innermost annulus is not seriously affected by blending. This is not surprising since C stars are among the brightest stars in the galaxy.

The average luminosity of the 47 C stars is $\langle I \rangle = 22.54$. Figure 5 shows their location on a close-up of the CMD. Nearly all of them, as expected, are brighter than the TRGB. For the

adopted distance and reddening this magnitude corresponds to $\langle M_I \rangle = -4.71$, a value similar to those found in other dwarf galaxies (Battinelli & Demers 2005b).

4.2. The C/M ratio in DDO 190

We shall deal only with the DDO 190 annulus defined in Sect. 3.1 since, as explained in that section, in the inner region crowding is severe and beyond the annulus the foreground/background contribution to star counts is dominant

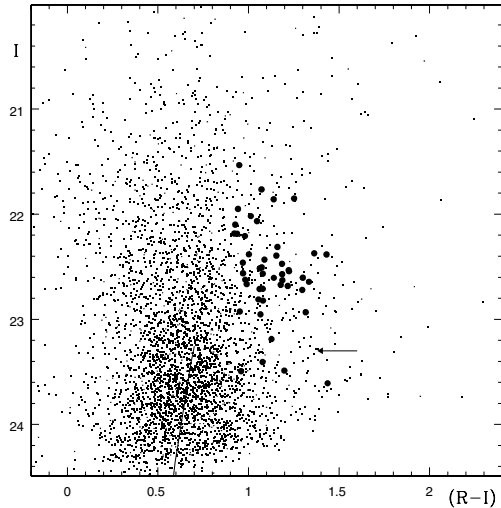


Fig. 5. A close-up of the CMD of the whole field with C stars shown as black dots. The arrow indicates the luminosity of the TRGB. The thick line represents the 12 Gyr isochrone for $Z = 0.001$ (Girardi et al. 2000).

with respect to the signal of the galaxy. To estimate the number of AGB M stars in the DDO 190 annulus we adopt the criterion described by Battinelli et al. (2003), i.e. we select those stars in the M-box of the colour-colour diagram with $M_{\text{bol}} < -3.5$. Bolometric magnitudes are computed using the Battinelli & Demers (2005a) bolometric corrections based on Bessell et al. (1998). In this region we count 33 M AGB candidates. In a $250 \text{ px} \times 1000 \text{ px}$ strip located on the South-East corner of the observed field we find 7 stars satisfying the same criterion. Taking into account the ratio between the annulus and the strip areas we conclude that the foreground/background contamination in the annulus is 18.1 stars and therefore we have 14.9 M AGB stars that belong to DDO 190. The number of C star in the annulus is straightforwardly given by the count of stars in the upper box in the colour-colour plot. Indeed, the foreground contamination for cool C stars in the galactic halo is essentially nil. We count 37 C stars in the DDO 190 annulus. Therefore, taking into account the statistical errors (as square-root of the numbers) on the C and M AGB star numbers determined above, we obtain $C/M = 2.5 \pm 1.0$.

In principle the number of C and M stars should be corrected for their different completeness levels. Indeed, C stars are generally “bolometrically brighter” than M stars and one may naively conclude that the former are more complete. Actually, the bolometrically brightest C stars tend to be very red and therefore heavily dimmed in R . This aspect was efficiently investigated by Brewer et al. (1995) who – by adding artificial C and M stars on the four V , I , CN and TiO frames – found for their dataset that the net effect of the incompleteness variation on the C/M ratio is small.

In order to assess the effects of incompleteness in our own dataset on the C and M star counts, we adopted a similar artificial star approach. First, we randomly selected 20 x, y positions within the annulus (i.e. the region used for the C/M ratio estimate). We then created four files of artificial stars with instrumental i, r, CN , and TiO magnitudes corresponding essentially

Table 3. Results of the artificial star tests: comparison of input and output magnitudes.

Filter	C stars	M stars
	$\Delta \pm \sigma$	$\Delta \pm \sigma$
I	-0.002 ± 0.065	$+0.024 \pm 0.077$
R	-0.002 ± 0.106	-0.021 ± 0.114
CN	-0.007 ± 0.061	$+0.016 \pm 0.058$
TiO	$+0.020 \pm 0.059$	-0.063 ± 0.105

to the observed magnitudes of our C stars. The artificial C stars were then added to the 40 images (11 I , 11 R , 9 CN and 9 TiO) which were processed by DAOPHOT/ALLFRAME. The M artificial stars were also processed in the same way using 40 individual fake images.

We therefore determine the recovery rate for both sets. We recover 20 of the 20 C stars (in the four filters), two of them show large (~ -0.3) differences between the input and output magnitudes, suggesting a significant blending for these stars. Their colours put them marginally outside of the C box. We recover 19 of the 20 M AGB stars, two of them are now too blue to satisfy our acceptance criteria and two others have slightly positive CN–TiO, not enough to be called C stars however. We therefore conclude that our recovery rates are 18/20 and 15/20 for C and M AGB stars respectively. Taking these numbers into account, the corrected C/M becomes 2.1. Similarly to the Brewer et al. conclusions, the correction we found is smaller than the statistical uncertainty of the raw C/M ratio.

These tests also permit us to estimate the effect of crowding, at the magnitude level of the AGB stars. Table 3 shows that crowding effect, for these bright stars, is relatively small.

Our tests show that we lose stars because their output colours are shifted outside the definition boxes. Obviously, some bluer M stars could be shifted to the red into the M-box. We did not introduce such artificial stars to investigate this aspect of the completeness.

4.3. The metallicity of DDO 190

The idea that the number ratio between the C and M stars might be anti-correlated with the metal abundance dates from the late seventies (Blanco et al. 1978). This anti-correlation is qualitatively well explained from the theoretical point of view by two facts: 1. It is easier to transform an O-rich star into a C-rich star when there is little oxygen to start with; 2. The giant branch of metal poor systems is steeper – and therefore bluer – than the metal-rich one, thus there are few if any M stars in very metal poor systems. For this reason the C/M has been often proposed as an easy observational proxy for the metallicity. However, the use of C/M to estimate the metallicity of stellar systems was hampered by the difficulties in obtaining a reliable empirical $[\text{Fe}/\text{H}] - \log(C/M)$ relation from collections of data available in the literature. Battinelli & Demers (2005a) presented an accurate calibration of this relation using a homogeneous dataset consisting exclusively of C and

M stars identified with the same criteria based on the $(R - I)$ and $(\text{CN} - \text{TiO})$ colours. We can thus convert the C/M obtain in the previous section into a metallicity estimate for DDO 190 that is a quite metal poor system with $[\text{Fe}/\text{H}] = -1.55 \pm 0.12$ ($[\text{Fe}/\text{H}] = -1.51 \pm 0.12$ for the completeness corrected C/M). Hidalgo-Gómez & Olofsson (2002) quotes an oxygen abundance of H II regions of $12\log(\text{O}/\text{H}) = 8.01 \pm 0.03$, a value revised to 7.74 by Pilyugin (2001) which translates into $[\text{Fe}/\text{H}] = -1.45$ using Maciel's (2001) relationship.

4.4. The shape of DDO 190

The first step in the investigation of the stellar surface density distribution of DDO 190 is to pinpoint the centre of the distribution. The x_c and y_c of the galaxy is determined from the centre of symmetry of the star counts versus pixel distributions for various 100 pixel wide strips oriented along the x and y axes. We estimate that we locate the centre within 10 pixels.

The $\sim 10\,000$ stars of the combined R images (no sharpness cutoff) are used to evaluate the shape of DDO 190. Two approaches are considered, one using star counts and the other one using the IRAF *isomap* task. Stars are counted, as a function of the distance to centre in 25 pixel bins, in 100 pixel wide strips of various orientations. The values of r for a given surface density is then noted for each orientation. Polar plots of these values reveal that the stellar distribution is well represented by a circle for $r = 350$ and 450 pixels. For larger distances we sample nearly exclusively the foreground/background objects. We conclude that DDO 190 appears circular to 2 arcmin from its centre.

The fact that we obtain off centre images of DDO 190 introduces border effects that complicate the determination of its symmetry to large distances. The IRAF *isomap* task leads to isodensity contours that are not perfectly circular. Indeed, we find a mean ellipticity, $\epsilon = 1 - b/a$, of 0.10 for contours with semi-major axes ranging from $2'$ to $3.5'$. Similarly to what was found by Aparicio & Tikhonov (2000) the position angle of the semi-major axis of the isophotes varies with radial distance to settle to about 90° in the outer region of the galaxy. Since the ellipticity is always very small, for simplicity we adopted a circular symmetry for DDO 190.

4.5. The profile of DDO 190

The dataset used in the previous sub-section reaches an instrumental magnitude $r = 18$, corresponding roughly to $R = 25$. Some radial variation of the incompleteness is expected. In order to evaluate such variation that would affect the slope of the density profile we performed an artificial star test by adding 200 stars randomly distributed over the frame and with magnitudes evenly distributed in the range (19.5, 25). Since we need to assess the recovery rate as a function of both radial distance and stellar brightness a large enough number of trials is necessary. We therefore repeated this addstar test 20 times for a total of 4000 added stars. The ratio between the recovered and added stars at different radial distances (1 arcmin radial binning) and

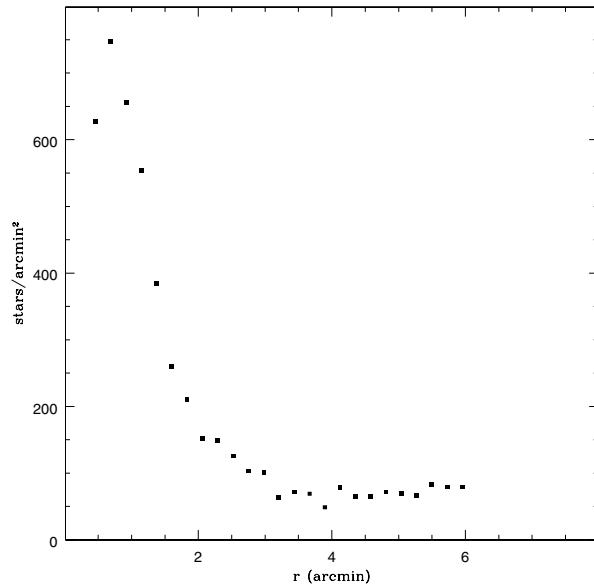


Fig. 6. Surface density profile of DDO 190 and its surrounding field. The counts are corrected for incompleteness.

in each magnitude bin (0.5 mag wide) is then computed. Our results indicate that:

- 1) In the innermost $1'$ the recovery rate remains higher than 80% for stars brighter than 22 mag and rapidly drops to nearly 0% for fainter objects. A clear bin-jumping from faint magnitude bins to brighter ones is evident, confirming severe blending. As a consequence, the average ($m_{\text{add}} - m_{\text{Rec}}$) is large and positive ($\Delta m = 0.35$). We note therefore that the magnitudes and colours of the few C stars in this region are quite uncertain.
- 2) In the region $1' < r < 3'$ the recovery rate starts to decline at $R \approx 22.5$ to reach 40% at $R \approx 23.5$ and then drops to almost zero. The average Δm is +0.06 and -0.07 in the inner and outer halves of this region. A moderate bin-jumping is appreciable in the inner half.
- 3) For $r > 3'$ the recovery rates in the 23.5 mag bin range from 50% to 70% but remain always lower than 20% for fainter magnitudes.

In the light of the above results, to avoid too large completeness correction factors, we limit our counts to stars $R < 24$ and $r > 1'$. We then correct the LF of observed stars in each of the 50 pixel wide annuli, taking into account the recovery results described above. These corrected counts are shown in Fig. 6.

4.6. The radial scale length and the extent of DDO 190

Figure 7 presents the logarithm of the density, with the foreground/background density subtracted. A least square through the points (with $r > 1'$) shown by the line yields a scale length $\alpha = 40'', \pm 5''$ a value identical to the scale length determined by Aparicio & Tikhonov (2001) using a shorter radial distance. This scale length is much larger than the one determined by Bremnes et al. (1999) from surface photometry.

The expected C star population of DDO 190 can be evaluated from its luminosity ($M_V = -14.5$). The Battinelli & Demers (2005b) relation yields ~ 120 C stars. This is more

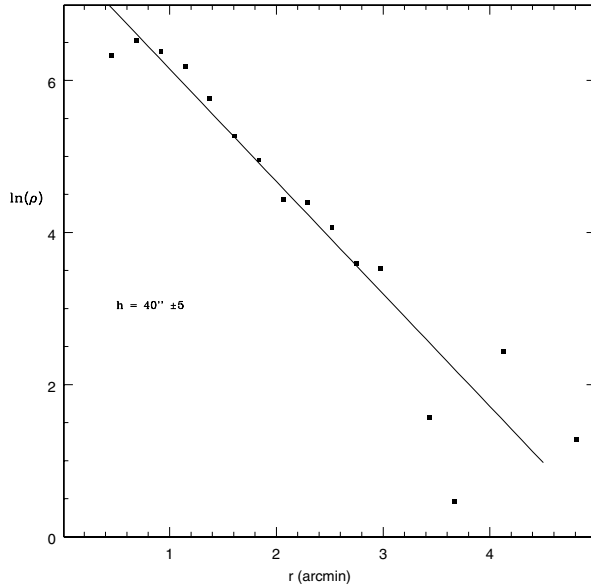


Fig. 7. The surface density of DDO 190 can be fitted to an exponential. The dashed line is the least-square fit to the points in the shown interval.

than twice the number identified. Obviously, many C stars were missed in the very crowded central region. Assuming that the C star density profile follows the profile of the giants shown in Fig. 7 (too few C stars are available to reliably determine the slope of the surface density gradient) we estimate that there should be nearly 100 C stars in DDO 190. The same density profile predicts 3.8 C stars with $r > 2'$: we count five of them.

Acknowledgements. This research is funded in part (S. D.) by the Natural Sciences and Engineering Research Council of Canada. It is a pleasure for us to thank the TNG staff for the valuable assistance and Marco Pedani for providing us with the transformation equations.

References

- Albert, L., Demers, S., Zijlstra, A. A., & Kunkel, W. E. 2000, *AJ*, 119, 2780
- Aparicio, A., & Gallart, C. 1995, *AJ*, 110, 2105
- Aparicio, A., & Tikhonov, N. 2000, *AJ*, 119, 2183
- Battinelli, P., Demers, S., & Letarte, B. 2003, *AJ*, 125, 1298
- Battinelli, P., & Demers, S. 2005a, *A&A*, 434, 657
- Battinelli, P., & Demers, S. 2005b, *A&A*, 442, 159
- Bessell, M. S., Castelli, F., & Plez, B. 1998, *A&A*, 337, 321
- Blanco, B. M., Blanco, V. M., & McCarthy, M. F. 1978, *Nature*, 271, 638
- Bremnes, T., Binggeli, B., & Prugniel, P. 1999, *A&AS*, 137, 337
- Brewer, J. P., Richer, H. B., & Crabtree, D. R. 1995, *AJ*, 109, 2480
- Davidge, T. 2003, *AJ*, 125, 3046
- Demers, S., Battinelli, P., & Letarte, B. 2004, *A&A*, 424, 125
- Dolphin, A. E. 2000, *PASP*, 112, 1383
- Girardi, L., Bressan, A., Bertelli, G., & Chiosi, C. 2000, *A&AS*, 141, 371
- Hidalgo, S. L., Marín-Franch, A., & Aparicio, A. 2003, *AJ*, 125, 1247
- Hidalgo-Gómez, A. M., & Olofsson, K. 2002, *A&A*, 389, 836
- Hudon, J. D., Richer, H. B., Pritchett, C. J., et al. 1989, *AJ*, 98, 1265
- Karachentsev, I. D., Sharina, M. E., Makarov, D. I., et al. 2002, *A&A*, 389, 812
- Letarte, B., Demers, S., Battinelli, P., & Kunkel, W. E. 2002, *AJ*, 123, 832
- Maciel, W. J. 2001, *New Astron. Rev.*, 45, 571
- Minniti, D., & Zijlstra, A. A. 1996, *ApJ*, 467, L13
- Minniti, D., & Zijlstra, A. A. 1997, *AJ*, 114, 147
- Minniti, D., Zijlstra, A. A., & Alonso, M. V. 1999, *AJ*, 117, 881
- Minniti, D., Borissova, J., Rejkuba, M., et al. 2003, *Science*, 301, 1508
- Mould, J. 2005, *AJ*, 129, 698
- Prugniel, P., & Héraudeau, P. 1998, *A&AS*, 128, 299
- Schlegel, D., Finkbeiner, D., & Davis, M. 1998, *ApJ*, 500, 525
- Stetson, P. B. 1994, *PASP*, 106, 250
- Stil, J. M., & Israel, F. P. 2002a, *A&A*, 389, 29
- Stil, J. M., & Israel, F. P. 2002b, *A&A*, 389, 42
- Vansevicius, V., Arimoto, N., Hasegawa, T., et al. 2004, *ApJ*, 611, L93